



# Satellite-derived bathymetry in optically complex waters using a model inversion approach and Sentinel-2 data

Gema Casal<sup>a,f,\*</sup>, John D. Hedley<sup>b</sup>, Xavier Monteys<sup>c</sup>, Paul Harris<sup>d</sup>, Conor Cahalane<sup>e</sup>, Tim McCarthy<sup>a</sup>

<sup>a</sup> National Centre for Geocomputation, Maynooth University, Maynooth, Co. Kildare, Ireland

<sup>b</sup> Numerical Optics Ltd, Tiverton, United Kingdom

<sup>c</sup> Geological Survey Ireland, Dublin, Ireland

<sup>d</sup> Sustainable Agriculture Sciences, Rothamsted Research, North Wyke, Devon, United Kingdom

<sup>e</sup> Department of Geography, Maynooth University, Maynooth, Co. Kildare, Ireland

<sup>f</sup> Faculty of Sciences, University of A Coruña, Campus da Zapateira, C/Rúa da Fraga, 10, 15071, A Coruña, Spain

## ARTICLE INFO

### Keywords:

Bathymetry  
Atmospheric correction  
Model inversion  
Coastal monitoring

## ABSTRACT

This study presents an assessment of a model inversion approach to derive shallow water bathymetry in optically complex waters, with the aim of both understanding localised capability and contributing to the global evaluation of Sentinel-2 for coastal monitoring. A dataset of 12 Sentinel-2 MSI images, in three different study areas along the Irish coast, has been analysed. Before the application of the bathymetric model two atmospheric correction procedures were tested: Deep Water Correction (DWC) and Case 2 Regional Coastal Color (C2RCC) processor. DWC outperformed C2RCC in the majority of the satellite images showing more consistent results. Using DWC for atmospheric correction before the application of the bathymetric model, the lowest average RMSE was found in Dublin Bay (RMSE = 1.60, bias = -0.51), followed by Mulroy Bay (RMSE = 1.66, bias = 1.30) while Brandon Bay showed the highest average error (RMSE = 2.43, bias = 1.86). However, when the optimal imagery selection was considered, depth estimations with a bias less than 0.1 m and a spread of  $\pm 1.40$  m were achieved up to 10 m. These results were comparable to those achieved by empirical tuning methods, despite not relying on any in situ depth data. This conclusion is of particular relevance as model inversion approaches might allow future modifications in crucial parts of the processing chain leading to improved results. Atmospheric correction, the selection of optimal images (e.g. low turbidity), the definition of suitably limited ranges for the per-pixel occurrence of optical constituents (phytoplankton, CDOM, backscatter) and seabed reflectances, in combination with the understanding of the specific characteristics at each particular site, were critical steps in the derivation of satellite bathymetry.

## 1. Introduction

Bathymetric information is essential in many coastal applications such as environment, management, research or economy. However, many shallow water areas worldwide remain unmapped. Coastal zones are under continuous pressures (e.g. human-induced alterations, erosion, storms) that can be enhanced by climate change effects (Halpern et al., 2008; Lipiec et al., 2018; Gamito et al., 2019). For this reason, maintaining detailed and updated information under these circumstances requires efficient technologies that can register these continuous changes. Precise bathymetric data are also necessary to

reach the SDG 14: Life below water of the Agenda 2030 for Sustainable Development (Wölf et al., 2019).

In the case of Ireland, much progress in the seafloor mapping has been achieved through the INFOMAR programme, the successor to the Irish National Seabed Survey (INSS). Between 1999 and 2005 the INFOMAR programme generated seafloor maps of more than 80% of Ireland's seabed territory involving a mapping coverage of 432,000 km<sup>2</sup>. Currently, the INFOMAR programme aims to cover the remaining unmapped areas, which mainly correspond with shallow coastal regions. Covering these areas with oceanographic vessels or small boats with acoustic equipment on board is not operative or involve associated

\* Corresponding author. National Centre for Geocomputation, Maynooth University, Maynooth, Co. Kildare, Ireland  
E-mail address: [gema.casal@udc.es](mailto:gema.casal@udc.es) (G. Casal).

<https://doi.org/10.1016/j.ecss.2020.106814>

Received 1 March 2020; Received in revised form 28 April 2020; Accepted 29 April 2020

Available online 6 May 2020

0272-7714/Crown Copyright © 2020 Published by Elsevier Ltd. All rights reserved.

navigational hazards. In this sense, optical satellite data can be an efficient alternative for bathymetric derivation in shallow coastal waters, providing temporal and spatial continuity. The potential of remote sensing to extract bathymetry has been recognised in clear shallow waters (<30 m) worldwide (Dekker et al., 2011; Eugenio et al., 2015). In Ireland, several attempts to characterize these zones using LiDAR (Coveney and Monteys, 2011) and multispectral satellite data (Monteys et al., 2015; Cahalane et al., 2019) have been made. However, the inherent conditions of Irish waters with high turbidity in some areas together with a high percentage of cloud coverage have often compromised the results obtained.

Sentinel-2 mission, with Sentinel-2A and Sentinel-2B registering data at 10 m of spatial resolution and a nominal revisit time of 5 days, offers new potential for coastal applications where satellite-derived bathymetry is included. These unique technical characteristics of Sentinel-2 have already been tested for bathymetry derivation in several locations worldwide. However, most of these studies have been performed in clear water environments (Traganos et al., 2018; Hedley et al., 2018; Evagorou et al., 2019) with only a few examples found in optically complex waters (Caballero et al., 2019).

When using remote sensing data to extract bathymetry, we can differentiate three main techniques: empirical approaches, empirically-tuned physics based, and optimization-tuned physics inversion approaches. Empirical approaches such as machine learning are the newest methods and not commonly used (Sagawa et al., 2019). The empirically-tuned physics-based have the longest history and are still the most frequently used (e.g. Lyons et al., 2011; Pacheco et al., 2015). In these methods, water column contributions and light attenuation properties are empirically derived from the satellite images by regression with in situ depth data (e.g. nautical charts, echo-sounder data or LiDAR). However, water turbidity and the influence of the seafloor can limit the performance of these algorithms, and they can be location- or data-limited (Lee et al., 2001). The detection and monitoring of changes can be a challenge using empirically tuned algorithms due to the influence of water column conditions, for example in turbid areas (Dekker et al., 2011). However, recent works have reported potential strategies for identifying (Caballero et al., 2019) and even reducing turbidity impacts (Caballero and Stumpf, 2020).

Even more complex, the application of optimization solutions to the model inversion approaches are being consolidated (Brando et al., 2009; Hedley et al., 2009; Dekker et al., 2011; Collings et al., 2018). In this study, a specific variant of the model inversion method as described in Hedley et al., 2009, 2010 and 2018 and implemented in the software package IDA (<https://www.numopt.com/>) was used. Although the term “physics-based” is frequently used to describe this optimization approach, the most common empirically-tuned algorithms, are also based on the physics of light transmission within the water column. Truly empirical algorithms, such as machine learning methods, are developed quite differently, and are not widely used. The primary difference in the model inversion method is that instead of using in situ data for calibration, it constrains the optical properties of the system a priori to physically plausible values, but also allows them to vary at each pixel. The application of the model requires the specification of a range of optical properties of the water and the seafloor (Gao, 2009). Although analytical approaches can perform well with multispectral data (Hamlyton et al., 2015; Hedley et al., 2018) they have been mainly applied to hyperspectral data and also mainly focused in clear water environments (e.g. Goodman et al., 2008; Brando et al., 2009; Dekker et al., 2011). The optically complex waters around the Irish coast, which can vary from relatively clear waters to highly turbid depending on the area, constitute an excellent range for testing this approach in challenging environments. Model inversion methods require specifying the range of optical properties that could occur at the site (Lee et al., 1999) – in optically complex waters this range is potentially more extensive, and thus increases uncertainties in the inversion, especially when using multispectral data.

An important aspect that needs to be considered in both tuning approaches, empirical and optimization, is the atmospheric influence. Especially for model inversion methods, the correction of atmospheric effects is considered a critical step for obtaining accurate bathymetry data (Goodman et al., 2008; Hedley et al., 2012; Eugenio et al., 2017). At satellite altitude, up to 90% of the sensor-measured signal in blue wavelengths can be due to atmospheric and surface reflectance (Gordon and Morel, 1983). Hence, it is crucial to have an accurate atmospheric correction method. Currently, several atmospheric processors are available for Sentinel-2 data. In previous studies, carried out in Irish waters, we found that the Case 2 Regional Coast Colour processor (C2RCC) produced the highest linear relationships between ratios of log-transformed bands and in situ depth (Casal et al., 2019). For this reason, this processor is considered in this study for comparison with the deep water calibration (DWC) approach implemented in the IDA software (Hedley et al., 2018).

In summary, the main objectives of this study are to:

- 1) Assess the performance of a model inversion approach to derived bathymetry using Sentinel-2 data in a range of optically complex environments around the Irish coast.
- 2) Compare atmospheric correction approaches for satellite-derived bathymetry, specifically the Case 2 Regional CoastColour (C2RCC) method versus a deep water calibration (DWC) approach.
- 3) Identify the challenges and opportunities for this methodology across a range of coastal environments.
- 4) Provide general recommendations for the practical application of this approach.

## 2. Material and methods

### 2.1. Study area

Dublin Bay is located on the east coast of Ireland and presents a C-shape with an approximately 10 km entrance (Fig. 1). Dublin Bay is a macro-tidal estuary with a mean tidal range of 2.75 m (Dyer, 1973) and an intertidal zone of about 16 km<sup>2</sup> (Brooks et al., 2016). In general, the entire bay presents a relatively flat topography with vast areas of fine sand combined with small areas of rocks and pebbles (Brooks et al., 2016). High nutrient loads, the deposition of large quantities of organic matter and undergoing regular dredging influence the water column conditions (O’Higgins and Wilson, 2005). The phytoplankton spring bloom varies interannually between April and May and presents a mean chlorophyll range of 2.2–5.5 µg L<sup>-1</sup> (O’Boyle and Silke, 2010). Between May and September, chlorophyll concentrations reach occasional peaks higher than 10 µg L<sup>-1</sup> (O’Higgins and Wilson, 2005).

Mulroy Bay is a glacially derived embayment with frequent strong winds, situated on the northern coast of County Donegal (Fig. 1). The tidal range varies on average from ~3.7 m (neap to spring) at the mouth of the Outer Bay to ~1.4 m in Broadwater (Moreno-Navas et al., 2011). Bar Rocks and High Rock, exposed at low tide, are navigational hazards in the centre of the bay. Studies carried out in Mulroy Bay reported total chlorophyll concentrations to be small, ~2 µg L<sup>-1</sup>, for most of the year-round with only occasional peaks in February and March (>5 µg L<sup>-1</sup>) (Telford and Robinson, 2003). Mulroy Bay is one of the most intensively farmed areas in Ireland regarding aquaculture (Telford and Robinson, 2003). These activities affect its water quality conditions. However, this effect is more pronounced at the Broadwater and the Northwater, areas not considered in this study.

Brandon Bay, located on the west coast of County Kerry, presents broad sandy intertidal areas with dunes covered by saltmarsh vegetation and hosts one of the longest sandy beaches in Ireland (12 km). (Fig. 1). Plant species are typically scarce on the flats, although there are some eelgrass beds (*Zostera sp.*) and patches of green algae (e.g. *Ulva sp.* and *Enteromorpha sp.*). Brandon Bay is highly exposed to wave action. On the west side, the Owenmore River discharges into a sandy estuary

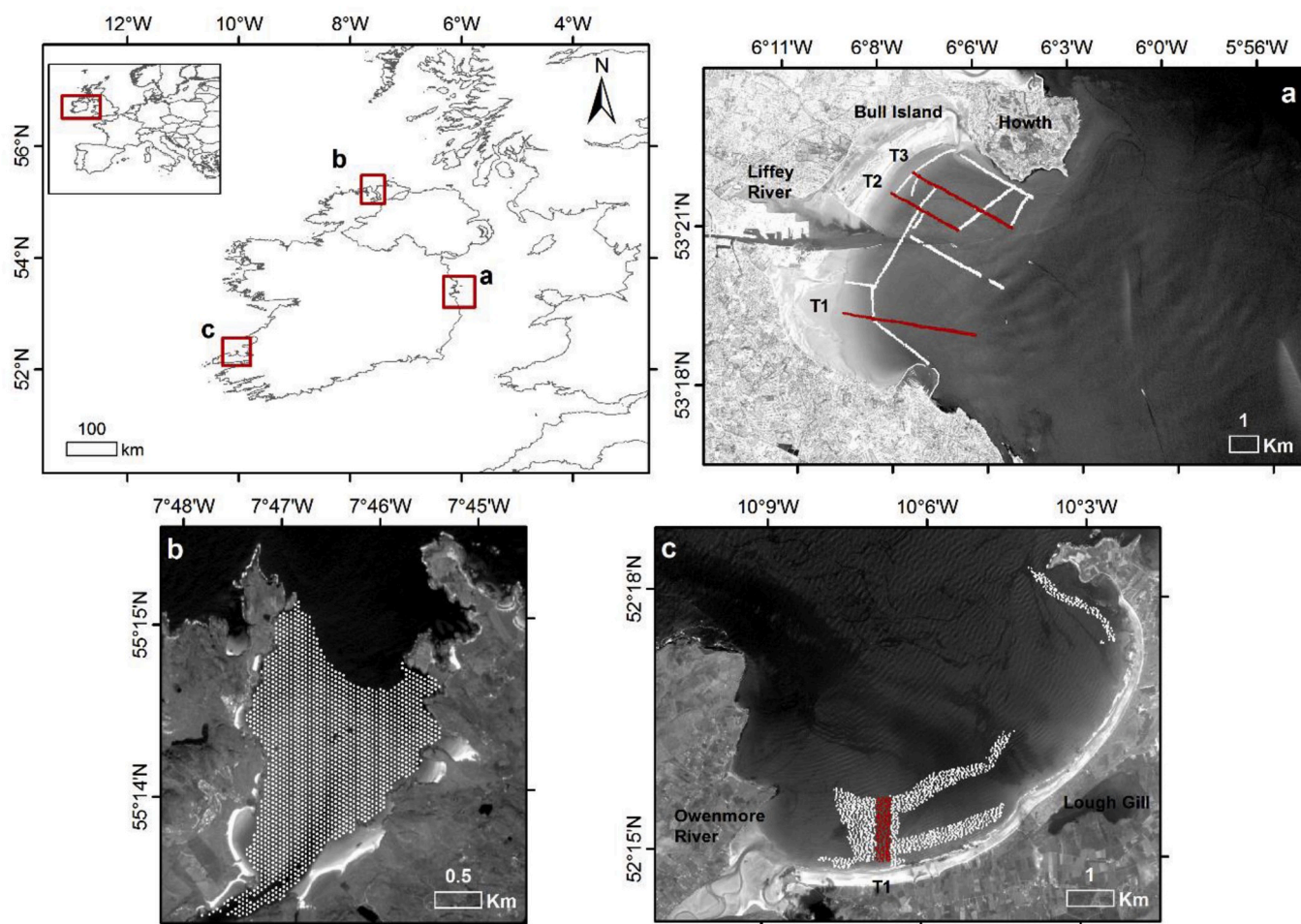


**Fig. 1.** Map of the study areas a) Dublin Bay b) Mulroy Bay and c) Brandon Bay. Overlapped are the multibeam data, of which the red points are transects referred to in the results (0 m–10 m). (For interpretation of the references to colour in this figure legend, the reader is referred to the Web version of this article.)

influencing the surface water conditions. Depending on the weather conditions, the discharge of this river produces high concentrations of sediments into the bay, especially on the western side. Brandon Bay is relevant for tourism and recreation, which have an economic and social contribution to the local community.

## 2.2. Field data

### 2.2.1. In situ depth

Several multibeam survey lines were acquired on the 25/07/2017 in Dublin Bay and processed using the hydrographic CARIS HIPSTM suite (Fig. 1). Vertical tidal corrections were applied and reduced to LAT (Lowest Astronomical Tide). Depth data meets International Hydrographic Organization (IHO) Order 1 standard. Multibeam bathymetric data for Brandon Bay were acquired between 25/09/2017 and 29/09/2017 using a Reson T-20 P multibeam system and processed using the same protocol and standards as for Dublin Bay. In the case of Mulroy Bay, the bathymetry data was acquired some years earlier, on the 11/09/2005 and 12/09/2005, using airborne LiDAR (Fig. 1). Vertical tidal corrections were also applied and reduced to LAT. Position uncertainty was less than 1 m, and the vertical error uncertainty was approximately 0.5 m. The horizontal spatial resolution of the un-gridded data is circa 4 m × 4 m. In all the cases, the data were gridded to 5 m × 5 m using an inverse distance weighted (IDW) algorithm and subsequently randomly reduced to approximately 2000 data points to optimise computing procedures. Only water depths between 0 and 10 m were considered for the subsequent analysis.

### 2.2.2. Bottom reflectance data

In the model inversion analysis, bottom reflectance is included as a linear mix of any pair of two endmember reflectance spectra drawn from a set of input spectra (an approach employed by several of the methods described in Dekker et al., 2011). For this reason, field campaigns to obtain measurements of sediment reflectance were carried out in the three study areas: Dublin Bay (03/10/2017; 23/05/2018; 25/05/2018), Brandon Bay (26/05/2018; 27/05/2018) and Mulroy Bay (04/06/2018). Spectra measurements were registered using a field spectroradiometer GER1500 at low tide and around noon-time when possible. A reference panel of 99% reflectance was used for calibration. Measurements were taken under stable atmospheric conditions and with an interval of less than 1 min between reference and target. Spectral signatures of the most representative intertidal substrates: sand, pebbles, rock, green and brown macroalgae were registered between 282 and 1092 nm with approximately 3.2 nm of spectral resolution (Fig. 2). The model inversion analysis is designed to perform all calculations at 2 nm intervals and convolve to Sentinel-2 bands as a final step. Therefore, the bottom spectral signatures were resampled to 2 nm resolution by linear interpolation as part of the model set up.

## 2.3. Satellite data

A total of 12 Sentinel-2 images were used, four for each study area (Table 1). The common presence of cloud cover, swell and sediment plumes considerably restrict the availability of suitable images over the Irish coast. Most of the images included in this study were free of clouds

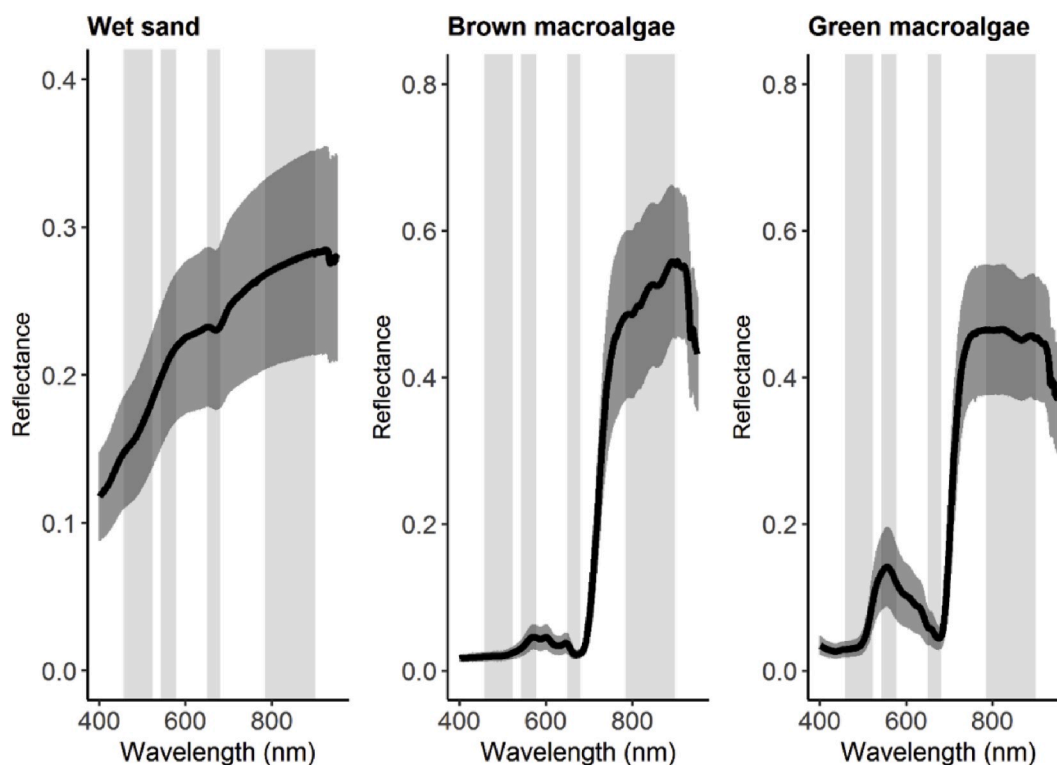


**Fig. 2.** Spectral signatures of benthic substrates: wet sand ( $n = 22$ ), brown macroalgae ( $n = 20$ ) and green macroalgae ( $n = 7$ ) measured in Mulroy Bay. Black line represents the average values and the grey vertical lines correspond to  $\pm$  standard deviation. Vertical boxes represent the wavelength range of the 10 m bands: B2 (458–523 nm), B3 (543–578 nm), B4 (650–680 nm) and B8 (785–900 nm).

**Table 1**

Detail of the Sentinel-2 images included in the study. Acquisition time is provided in Coordinated Universal Time (UTC); Note Irish Standard Time in summer is UTC+1. Tide height (m) information was provided by the Irish National Tide Gauge Network. Wind speed ( $\text{m s}^{-1}$ ) was taken from Dublin Bay Buoy for Dublin Bay, Foyle Buoy for Mulroy Bay and Ballybunnion Buoy for Brandon Bay. These buoys are part of the meteorological and oceanographic (MetOcean) sensors network.

Study area	Satellite	S2-granule	Date	Acquisition Time (UTC)	Tide Height (m)	Wind speed ( $\text{m s}^{-1}$ )
Dublin Bay	S2-A	T29UPV	17/06/2017	11:33	1.29	3.60
	S2-A		17/07/2017	11:33	1.25	6.17
	S2-B		07/06/2018	11:33	1.75	3.08
Mulroy Bay	S2-B		05/09/2018	11:33	1.69	3.85
	S2-A	T29UNB	04/05/2017	11:54	2.51	6.68
	S2-A		20/06/2017	11:43	1.99	4.63
	S2-A		23/07/2017	11:43	0.57	3.09
Brandon Bay	S2-B		30/06/2018	11:43	1.49	6.17
	S2-A	T29UMT	11/05/2017	11:43	1.38	1.54
	S2-A		29/04/2018	11:54	0.72	3.60
	S2-A		29/05/2018	11:54	1.46	3.08
	S2-B		03/07/2018	11:53	0.22	5.66

and close to the optimal conditions as judged by visual inspection (low turbidity and low presence of white caps). Some images presenting sub-optimal conditions were also included for comparison. All the selected images exhibited sun glint to some extent. Moreover, the images registered over Dublin Bay were also affected by the change in the cross-track view direction of the MSI sensor units. This effect, due to different detector view angles (ESA, 2018), is nominal in Sentinel-2 imagery and is amplified when the levels of illumination from the sun are strongest on the eastern side of the image swath (see figures later). Only the 10 m resolution bands were included in the analysis. Band 1 (444 nm) was ruled out due to its low spatial resolution (60 m), and for consistency with previous studies (Casal et al., 2019, 2020).

Since model inversion methods work with water-leaving reflectance as a radiometric quantity, accurate atmospheric correction is essential and has a significant impact on the bathymetry results (Goodman et al., 2008). For this reason, before the bathymetric algorithm application, all

the Sentinel-2 images were atmospherically corrected using two different methods: 1) Case 2 Regional CoastColour processor (C2RCC) and 2) the Deep Water Calibration (DWC) method implemented in the IDA software (Hedley et al., 2018).

C2RCC (Doerffer and Schiller, 2007) relies on an extensive database of simulated water-leaving reflectance and related TOA radiances using neural networks. These neural networks determine the water-leaving radiance from the TOA and retrieve inherent optical properties of the water body (Brockmann et al., 2016). Outputs of remote sensing reflectance ( $R_{rs}$ ) defined as the ratio of water-leaving radiance to the total downwelling irradiance just above water were selected. This processor showed the best results in previous studies using empirically tuned algorithms and seems to reduce the presence of sun glint (Casal et al., 2019). For this reason, no sun glint correction was applied after the atmospheric correction using this processor.

DWC atmospheric correction is based on a set of look-up-tables for

atmospheric reflectance and transmission including a maritime 99% relative humidity aerosol model as described in Antoine and Morel (1999) and Shettle and Fenn (1975). The look-up-tables are generated by libRadtran (Emde et al., 2015) and are parameterised on solar-view geometry, with the only two free parameters being aerosol optical thickness,  $\tau(550)$  ranging between 0 and 0.3, and wind speed,  $u_{10}$ , ranging between 0  $\text{ms}^{-1}$  and 10  $\text{ms}^{-1}$  (conditions of the sea surface state). The main effect of these two parameters is to notionally contribute to a spatially homogenous component of atmosphere and indirect sea-surface reflectance, i.e. sky reflectance (Hedley et al., 2018). Per-pixel sun glint effects were first corrected using the regression-based deglint method (Hedley et al., 2005) using the band 8 (842 nm) with 10 m resolution corresponding to the NIR (Near Infra-Red) to estimate and correct the sun glint present in visible bands. After this step, the atmospheric correction estimates a value for the aerosol optical thickness and a value for wind-speed to be applied over the whole image area. This estimation was based on a set of deep water areas selected by the user, an inversion procedure finds the optimal solution for  $\tau(550)$  and  $u_{10}$  that results in deep water estimates in the bathymetric method (described below). Therefore, this atmospheric correction is tailored to the bathymetry model, and is perhaps better interpreted as an alignment of the image to the bathymetry model, rather than an independent atmospheric correction.

#### 2.4. Bathymetry mapping

The basis of the optimization method is a forward model of above-water spectral remote sensing reflectance  $R_{rs}(\lambda)$  based on parameters of the water column and bottom substrates reflectance. This combination of optimization with inversion was initially developed by Lee et al. (1998, 1999, 2001) and later modified by other authors (e.g. Hedley et al., 2009), following the general form :

$$R_{rs}(\lambda) \approx f(P, G, X, H, e_1, e_2, m, \lambda) \quad (1)$$

In equation  $P$ ,  $G$ ,  $X$  and  $H$  represent, respectively, the water column phytoplankton, the coloured dissolved organic matter (CDOM), particulate backscatter, and depth. The bottom reflectance is a linear mix of two endmember reflectance spectra drawn from a set of  $n_e$ , and indexed by  $e_1$  and  $e_2$  such as that  $0 \leq e_1, e_2 < n_e$ . The mix fraction of  $e_1$  vs  $e_2$  is given by  $m$  which ranges from 0 to 1. In this study, endmembers of wet sand, green macroalgae and brown macroalgae were included. At each pixel in the image a look-up table inversion procedure (Adaptive-Look-Up Tables, ALUT, Hedley et al., 2009) was applied to find the input values to the model which produced the closest spectral match to image reflectance. For the look-up-table approach bounded ranges for the different parameters were established. The limits of these ranges were defined taking into account previous studies carried out in Irish waters and similar areas (e.g. Lee et al., 1999; O'Higgins and Wilson, 2005; Bowers et al., 2013; Garaba et al., 2014) as well as taking into account the experience of the authors in the Irish coast and other areas. After testing several combinations, and in the absence of specific surveys to register these measurements, the limits were defined as follows: phytoplankton ( $P$ ) ranging between 0 and 10  $\mu\text{g L}^{-1}$  for Dublin Bay and Brandon Bay while for Mulroy Bay the range was defined between 0 and 2  $\mu\text{g L}^{-1}$ . The same range of CDOM ( $G$ ) absorption at 440 nm,  $a(440)$ , and particulate backscatter at 440 ( $X$ ),  $b_{bp}(440)$ , was used for the three study areas. These limits were from 0 to 0.3  $\text{m}^{-1}$  in the case of CDOM ( $G$ ) and from 0 to 0.2  $\text{m}^{-1}$  in the case of backscatter ( $X$ ). Only a range between 0 m and 10 m was included for depth estimations, partly because it was not expected to be able to produce deeper accurate estimates in these optically complex waters. Moreover, this depth range is the most challenging for boat-based survey techniques and where satellite-derived bathymetry offers the most potential complementary value.

The model inversion method provides per-pixel bathymetry uncertainty estimates (Hedley et al., 2010, 2018a). The uncertainty estimates

were calculated in the bathymetry derivation process but not explored in this study. However, the uncertainty propagation does affect the calculation of the bathymetry, so some details are relevant here. Uncertainty is propagated by inverting each pixel 20 times with a random spectral error term added to the pixel reflectance derived from the covariance matrix over a deep water area (Hedley et al., 2010, 2016). This error term, the environmental noise equivalent radiance,  $NE\Delta R_{rs}(\lambda)$  (Brando et al., 2009), notionally includes all sources of pixel-to-pixel variation from water surface upwards, which in the context of the model can be considered noise. Usually, this noise term is dominated by variable water surface reflectance (even after glint correction) but may also contain atmospheric fluctuations and instrument noise (Hedley et al., 2018). The best estimate for bathymetry at each pixel was taken as the mean over the 20 inversions. It should be noted, that typically, this mean estimate is slightly different to a single non-noise perturbed inversion estimate. Tide correction for the time of the image acquisition was applied using the data provided by the Irish National Tide Gauge Network mentioned in Table 1.

Validation of the results was performed by the comparison of the satellite-derived bathymetry and in situ depth (multibeam and LiDAR) data for each study area. A mean  $3 \times 3$  pixel filter was also applied to the retrieved bathymetric maps before validation procedures to smooth the data and reduce noise (Traganos et al., 2018; Hedley et al., 2018a; Casal et al., 2019). Coefficient of determination ( $R^2$ ), bias and Root Mean Square Error (RMSE) diagnostics were determined. These diagnostics were calculated for the total number of matchups (0–10 m) and for data binned every 2 m: 0–2 m, 2–4 m, 4–6 m, 6–8 m and 8–10 m.

$R^2$  is a statistical fit measure of how close the data are to a fitted regression line. A low  $R^2$  indicates that the model explains a low percentage of the variability of the response data around its mean. However,  $R^2$ , as taken in isolation, is not always a reliable indicator of accurate bathymetry and vice versa. The interpretation will depend on the behaviour of associated scatterplots and the ranges of depths. For example, a model with a low  $R^2$  could be due to poor fit in the overall range of 0 m–10 m but at the same time showing good performance in depths shallower than 5 m. The bias diagnostic determines the tendency to over- or under-estimate the in situ values (resulting in negative and positive bias values, respectively). The RMSE represents the difference between estimated values and observed values. Ideally, it should tend to zero. Bias and RMSE were defined as:

$$Bias = \sum_{i=1}^N \frac{\rho_{satellite} - \rho_{insitu}}{N} \quad (2)$$

$$RMSE = \sqrt{\sum_{i=1}^N \frac{(\rho_{satellite} - \rho_{insitu})^2}{N}} \quad (3)$$

After the initial analysis, the individual transects indicated in Fig. 1 were subjected to a more detailed inspection. In this case, in addition to the bias (Eq. (2)) the 'spread' was calculated being the width of the interval around the bias-corrected 1:1 line within which 90% of the points lie. I.e. the spread metric is equivalent to saying that 'the results when corrected for a systematic bias of  $X$  m were within  $\pm Y$  m of the in situ data 90% of the time', where  $Y$  is the spread. This process facilitates a straightforward expression of the performance and the separation of bias (accuracy) from spread (precision).

### 3. Results and discussion

#### 3.1. Evaluation of atmospheric correction methods

Analysis of the 12 Sentinel-2 images confirmed that atmospheric correction influences the accuracy of bathymetric values derived from satellite data. Scatterplots showed that using DWC method 9 of the 12 images presented higher  $R^2$  values, and 10 presented lower RMSE than

using C2RCC processor (Fig. 3 and Fig. 4). A clear relationship between satellite-derived depth and in situ depth was evident in all the scatterplots except for the image for the Dublin bay image of September 5, 2018 (Figs. 3d and 4d) due to high turbidity conditions present in the image (discussed below). The scatterplots resulting from C2RCC atmospheric correction also showed a saturation of satellite-derived depths at lower values than the DWC processor (e.g. Figs. 3b and 4b). For these reasons, DWC was considered the preferred atmospheric correction and the remaining analysis of the bathymetric results presented here will mainly refer to this processor.

### 3.2. Site and image-specific impacts on bathymetry estimation

For either atmospheric correction, analysis of the scatterplots of satellite-derived depth against in situ data confirms that the environmental conditions present in the Sentinel-2 image influences in great extent the performance and accuracy of the model inversion. For example, Figs. 3d and 4d correspond to a Sentinel-2 image with high turbidity as a consequence of the high waves and heavy rain produced by the subtropical storm Ernesto (18th-19th August 2018). In this case, there was almost no meaningful relation between satellite-derived depth and in situ depth regardless of the atmospheric correction used. Storm events are frequent in Ireland affecting water quality conditions and therefore satellite bathymetry derivation. The effects of light turbidity were also visible in other scatterplots (e.g. Figs. 3j and 4j) resulting in a wider scatter in the relationship between the satellite signal and depth.

Evaluating the results in more optimal conditions, scatterplots corresponding to Dublin Bay (Fig. 4 a-c) and Mulroy Bay (Fig. 4 e-g) appeared closer to the ideal 1:1 line with higher  $R^2$  values. This result was expected for Mulroy Bay as it has the highest water transparency conditions of the three study areas considered (Casal et al., 2019). However, despite its optically complex waters, where optimal conditions were present (e.g. very low turbidity), results in Dublin Bay were better than the ones obtained in Mulroy Bay (up to 10 m water depth), showing higher  $R^2$  and lower RMSE values. The surface water conditions present in Brandon Bay are more complex. Brandon Bay is an open bay, highly exposed to the wave action and has events of moderate turbidity, primarily due to the influence of the Owenmore River. These conditions, together with a steeper bottom slope, restrict the consistency of the satellite depth to in situ depth relationship and result, in general, in lower  $R^2$  values. For the three sites the optimal results, identified from inspection of the scatterplots and images together with RMSE, bias and  $R^2$  values, corresponded to the images acquired on the 17/07/2017, 23/07/2017 and 11/05/2017 for Dublin Bay, Mulroy Bay and the Brandon Bay, respectively (Fig. 4b, g, 4i).

Visual inspection of the scatterplots also revealed common features in all the study areas as well as particular conditions for each study site (Fig. 5). In some images, the effect of local turbidity events caused underestimates of bathymetry. For example, in Dublin Bay run-off coming from the saltmarshes of Bull Island produced shallower estimated depths between 1 m and 5 m in the northern part of the bay, close to the Howth peninsula (e.g. Fig. 5a). A number of points in the scatterplots of Brandon Bay and some of Mulroy Bay (Fig. 4) indicate areas where satellite-derived bathymetry produced deeper values than the in situ bathymetry. These areas appear to have a darker bottom type which produced an over-estimation of satellite-derived depth. In the case of Mulroy Bay these matchups were located in rocky bottom close to the shore and deeper areas of the river channel (Fig. 5 b); while in the case of Brandon Bay were located in the northern and middle part of the bay (Fig. 5c). Overall the results indicate the existence of various confounding characteristics particular to each study site that could be considered on a site by site basis. Understanding the specific features of a site is therefore important when applying satellite-derived bathymetry models.

From the analysis of the scatterplots, some negative values were found in very shallow waters. Since tidal corrections were applied, negative depths would be expected in places which are emergent at

lowest astronomical tides, i.e. anywhere in the intertidal zone. Bearing in mind these areas are submerged at the time of image acquisition, the negative values could also represent an underestimation of depth as compared to the multibeam or LIDAR data in shallow areas. Typically, the depth estimation in shallowest areas is very consistent (Fig. 5) so the question is how a systematic deviation can arise. Aside from potential radiometric (model-based) issues, one possibility is a local variable difference between the in situ depth data and the tide gauge used for the tide correction. In the case of Mulroy Bay and Brandon Bay, the tide gauge was not exactly in the study area. In Mulroy Bay, variations in sediment deposition could also have contributed to the deviation observed, between the satellite-derived depth and the in situ depth. Even Mulroy Bay is a stable area, a significant difference exists (~10 years) between the LIDAR data, used for validation, and the Sentinel-2 images. Another reason that could explain this discrepancy is the limitation of airborne LIDAR data in shallow areas to differentiate between water-surface return and the seafloor return. Regardless, these very shallow waters (<0.5 m) are not a priority for satellite-based surveying, being amenable to other survey methods (e.g. Unmanned Aerial Vehicles) and having a little impact for navigation or seabed morphology studies.

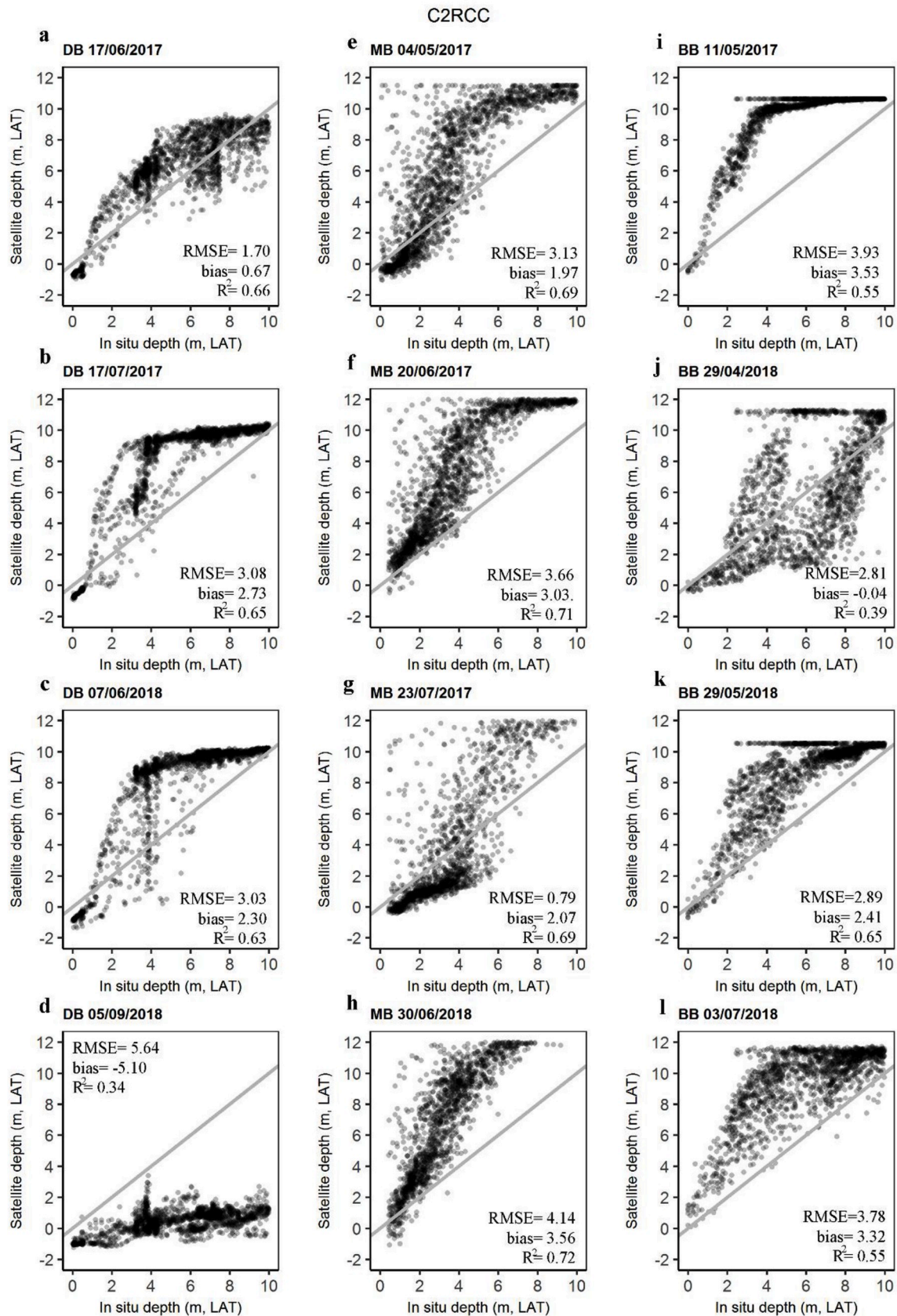
### 3.3. Accuracy, precision and consistency of bathymetric estimates

Fig. 6 summarises the bias, RMSE and  $R^2$  values at different depth ranges for the three images that were selected as the optimal results. Also shown are the average values over all images for different depth ranges. For each study area, one of the four images was excluded from the average calculation since meteorological or water column conditions were evidentially poor. In the case of Dublin Bay and Brandon Bay, the images ruled out corresponded to the ones registered on the 05/09/2018 and the 29/04/2018 respectively, both due to high turbidity. In the case of Mulroy Bay, the image ruled out was the one registered on the 30/06/2018, due to atmospheric haze affecting the area. These plots, therefore, indicate the best performance in the context of 'reasonably expected' good performance. In practice, the results from the single optimal images and three-best averages were very similar (Fig. 6).

Bias values for Dublin Bay showed variability being positive or negative depending on the depth range considered. In Mulroy and Brandon Bay, bias values were in both cases positive, indicating a tendency toward overestimation of satellite-derived depth. In general, bias was less for Dublin Bay in comparison with Mulroy Bay and Brandon Bay, Brandon Bay had the most significant bias values. Regarding the depth range, the largest bias values were found between 8 m and 10 m in the case of Dublin Bay but were less than 1 m in most of the depth ranges at that site. In Brandon Bay, the largest bias was found between 4 m and 8 m with values of ~3 m. Bias in Mulroy Bay showed similar values in all the depth ranges considered (<2 m).

Considering all the depth ranges, the highest RMSE values were found in Brandon Bay and showed almost no difference between the optimal image and the average (Fig. 6c). Dublin Bay presented the lowest RMSE values, and the optimal image and the three-best average presented very similar values up to depths of 6 m, beyond which the optimal image maintained consistent RMSE of ~1 m, but the three-best average RMSE increased (Fig. 6 a). This fact was an expected result because as errors are introduced they become significant in deeper areas first. RMSE in Mulroy Bay showed less variability between depth ranges being lower than 2 m when the optimal image is considered.

Before describing the  $R^2$  values, it should be reminded here that for a correct understanding of these values in SDB studies they should be interpreted together with RMSE and bias. Taking this issue into account,  $R^2$  values showed different behaviour between the study areas. In the case of Dublin Bay and Brandon, a loss of relationship between satellite and in situ depth was observed between 6 m and 8 m. For Mulroy Bay, the highest  $R^2$  values were also found between 0 m and 2 m with similar values in the rest of depth ranges considered ( $R^2 < 0.2$ ). In general,  $R^2$  values obtained over the whole depth range (Fig. 4) were much higher



**Fig. 3.** Scatterplots of satellite derived depth vs in situ depth. Atmospheric correction using C2RCC processor has been applied previously to the inversion approach. DB indicates Dublin Bay ( $n = 1628$ ), MB indicates Mulroy Bay ( $n = 1818$ ) and BB indicates Brandon Bay ( $n = 1591$ ). RMSE, bias, and  $R^2$  are included in each plot. The grey line represents the 1:1 regression line.

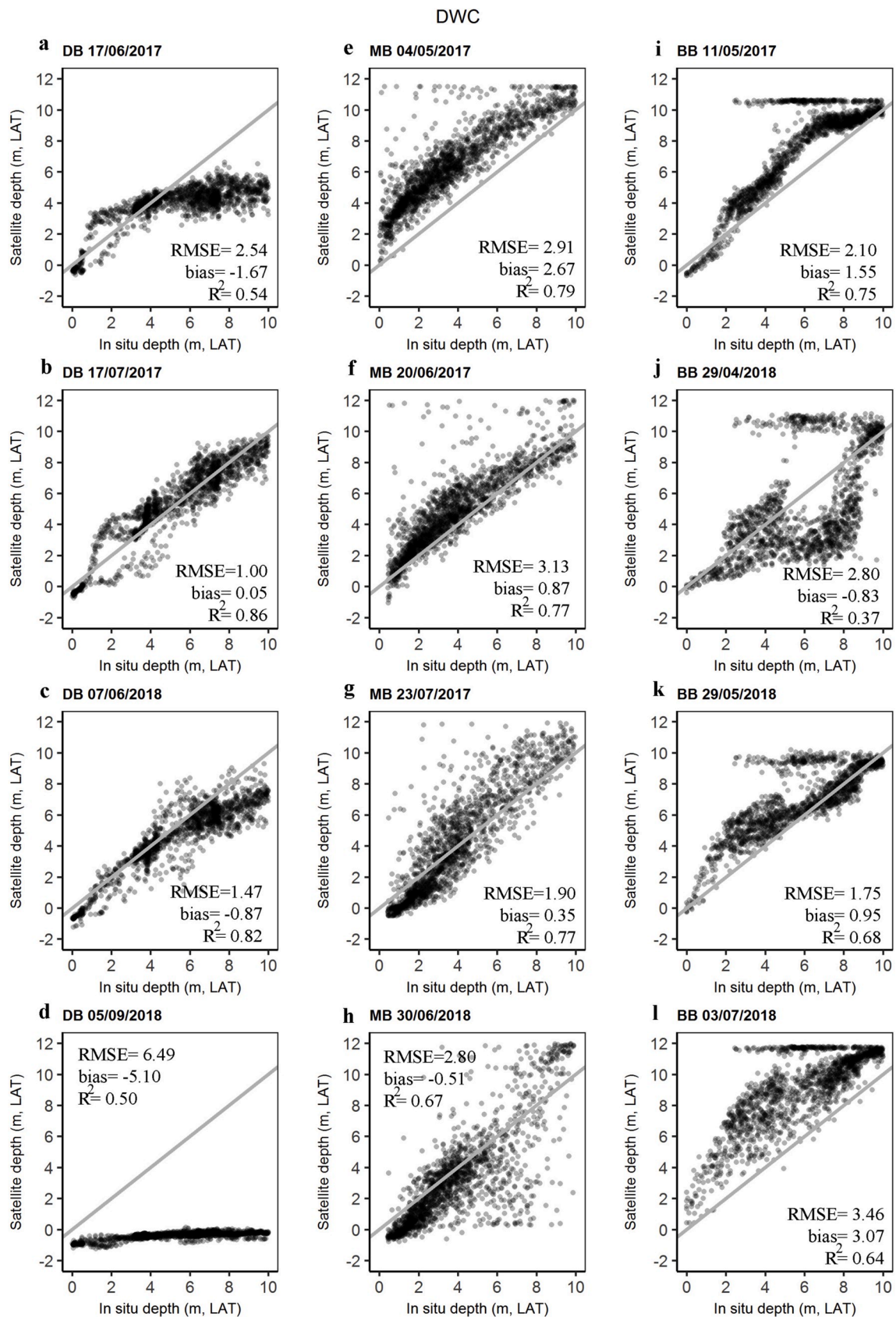


**Fig. 4.** Scatterplots of satellite derived depth vs in situ depth. Atmospheric correction using DWC processor has been applied previously to the inversion approach. DB indicates Dublin Bay (n = 1628), MB indicates Mulroy Bay (n = 1818) and BB indicates Brandon Bay (n = 1591). RMSE, bias, and R<sup>2</sup> are included in each plot. The grey line represents the 1:1 regression line.



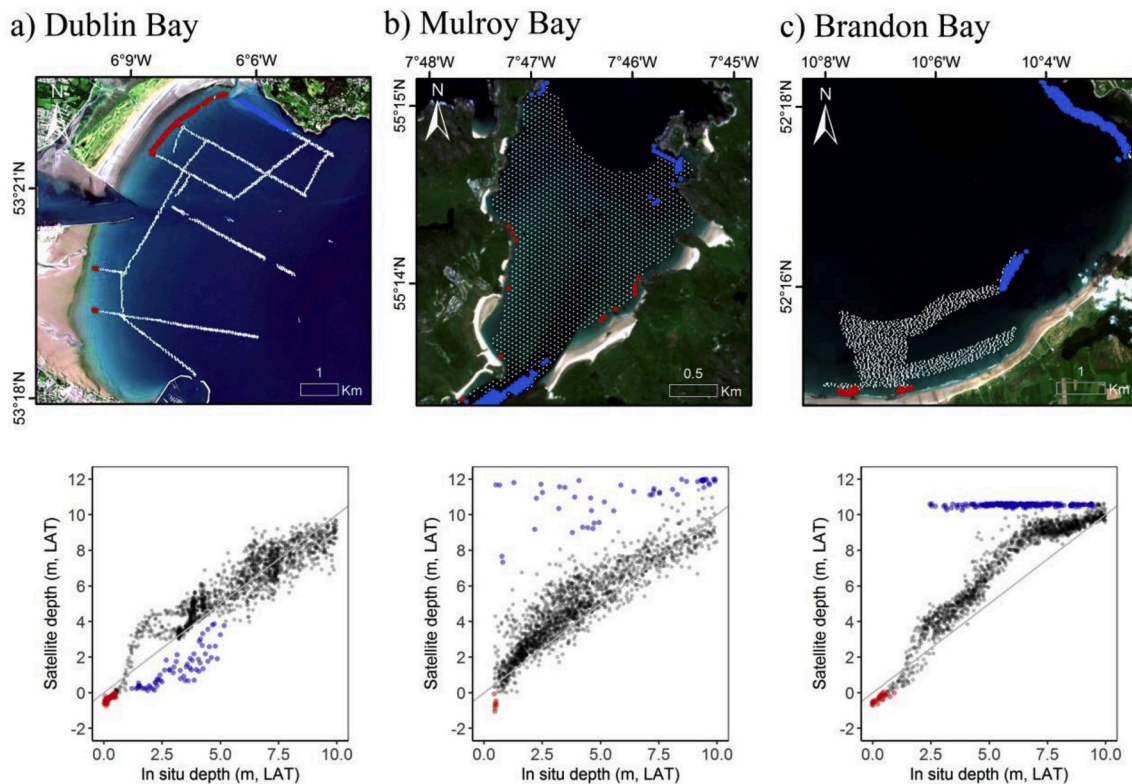


**Fig. 5.** Spatial distribution of “anomalous” satellite-derived depth values detected in the scatterplots. Red colour represents negative values, i.e. areas estimated as intertidal by satellite data but not by in situ data. Blue colour represents derivations of the model producing over-prediction and under-prediction of depth values. Sentinel-2 images (RGB) and the correspondent scatterplots for A) Dublin Bay (17/07/2017) b) Mulroy Bay (23/07/2017) and c) Brandon Bay (11/05/2017). (For interpretation of the references to colour in this figure legend, the reader is referred to the Web version of this article.)

than in the 2 m intervals, but this fact was especially evident in the case of Mulroy Bay. The broad-scale correspondence of depth estimates to in situ data over a range of 10 m is clearly better than in a subset 2 m interval, where data point noise becomes a more substantial factor. In summary, these results showed consistent error over all depths in Dublin Bay and Mulroy Bay, but greater variability in Brandon Bay.

The plots of Fig. 4 show the results over the entire site, but as shown in Fig. 5 outliers are spatially correlated. This fact implies there is a locality to the pattern of results that may also apply to the correspondence between data points and bathymetry estimates in regions of overall better performance. To understand spatial patterns, further individual localised transects were considered for Dublin Bay (T1, T2 and T3 in Fig. 1a) and Brandon Bay (T1 in Fig. 1c). Mulroy Bay was not considered due to the difference in time between the in situ data and the satellite images.

For the ‘best result’ Dublin Bay image of 17/07/2017 the bias on two transects, T1 and T3, was less than 0.5 m while for T2 was 0.69 m (representing overestimation of depth) (Fig. 7, centre column). The 90% confidence interval spread less than  $\pm 1.55$  m for all transects. For the other two images, bias was generally larger, but still variable between transects of the same image. In some cases, especially in the image of 17/06/2017 (Fig. 7 left column) the correspondence between in situ data and satellite estimates was curved, meaning the ‘bias’ not an especially useful metric. For Brandon Bay, similar observations were made, but in this case, the spread was more constant between images (Fig. 8). All bias values were positive in this case, indicating an overestimation of depth.

These results showed that satellite-derived depth is highly variable and depends on many factors. Systematic errors within an image, such as the curve in all three transects of the image taken on the 17/06/2017 (Fig. 7 a, d, g), could be attributed to image conditions or issues with atmospheric correction, since a radiometric discrepancy between the model and input image data may explain this result. Conversely,

systematic errors that occur in all images at specific spatial locations are site-dependent (e.g. Fig. 5). However, the situation is more complicated where there is reasonable adherence to a unity slope, but variation in bias within an image exists. For example, transect T2 in image 17/07/2017 has a bias of 0.69 m (Fig. 7e) but this bias is almost zero in transect T1 (Fig. 7b). The results along transect T2 are potentially influenced by the outflow of the Liffey River (Fig. 1). These results show that while the basic capability for estimating bathymetry over the 0–10 m range was very good, there can be local spatial influences within a single image that are not visually obvious, maybe thin aerosol plumes or variations in water constituents. It should, of course, be remembered that while in situ data is assumed ‘correct’ it might also be subject to spatial errors and change over time.

### 3.4. Bathymetric maps

The satellite-derived bathymetry maps (Fig. 9) obtained from the ‘optimal’ images with either C2RCC or DWC correction were representative of the actual known bathymetric features described by the INFOMAR programme and also by other studies carried out in the same areas (e.g. Monteys et al., 2015; Cahalane et al., 2017; Casal et al., 2019; Casal et al., 2020).

In the case of Dublin Bay, it was observed a progressive increment in depth from the shore to the outer areas and also from northern areas to southern areas. This difference was more evident in the image corrected by DWC (Fig. 9c). In both cases, C2RCC and DWC, the Liffey River channel was identified as a deeper area. To the East of the bay, the Burford and Kish sandbanks were visible also in both cases. However, they were more defined in the map resulting from DWC (Fig. 9c). The alternation of detectors in the along-track direction of the MSI had also an impact on the resulting bathymetric maps (Fig. 9c) however, given the pixel-to-pixel noise level in the bathymetry estimates was not a

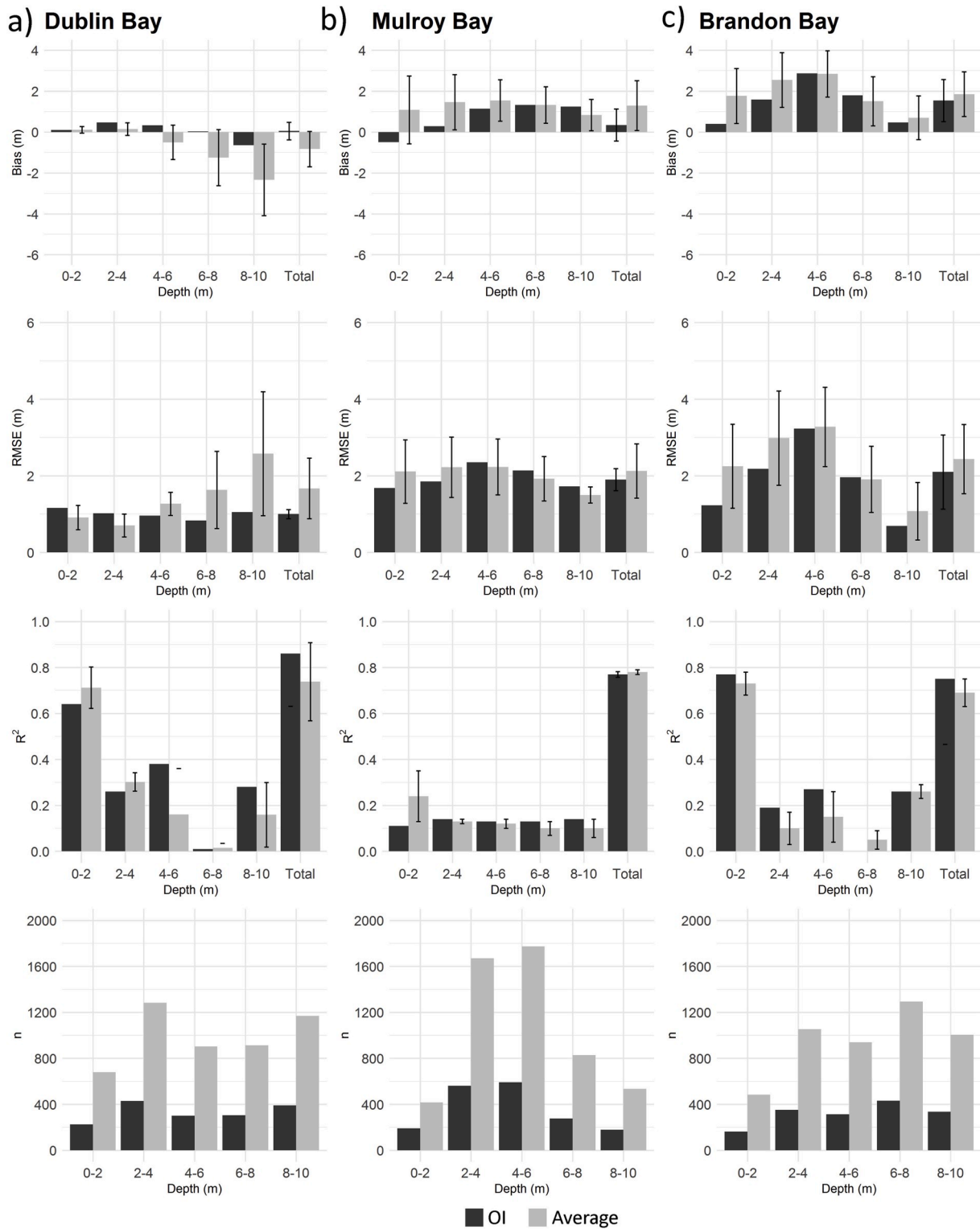


**Fig. 6.** Bias, RMSE, R<sup>2</sup> and n values resulting from the optimal images and the average of all the images considered by study area a) Dublin Bay, b) Mulroy Bay, c) Brandon Bay. n corresponds to the total number of matchups. Bar lines represent standard deviation and they are only shown in the case of average values. Some of the images have been ruled out because of meteorological and water column conditions. These images corresponded to the ones registered on the 05/09/2018, 30/06/2018 and 29/04/2018 for Dublin Bay, Mulroy Bay and Brandon Bay, respectively.

significant source of error (being not even visible in the transects in Fig. 7). This finding was consistent with previous studies which have reported that while this striping effect has an impact when visually examining the data, it does not significantly alter bathymetric values (Casal et al., 2019).

In Mulroy Bay, shallow areas were located close to the shores, with the western side deeper than the eastern side. The deepest values were located at the mouth of the bay and the inner channel. Rocky shallow areas in the central part of the bay were also reflected in the bathymetric maps. In the case of Brandon Bay, bathymetric maps showed a more

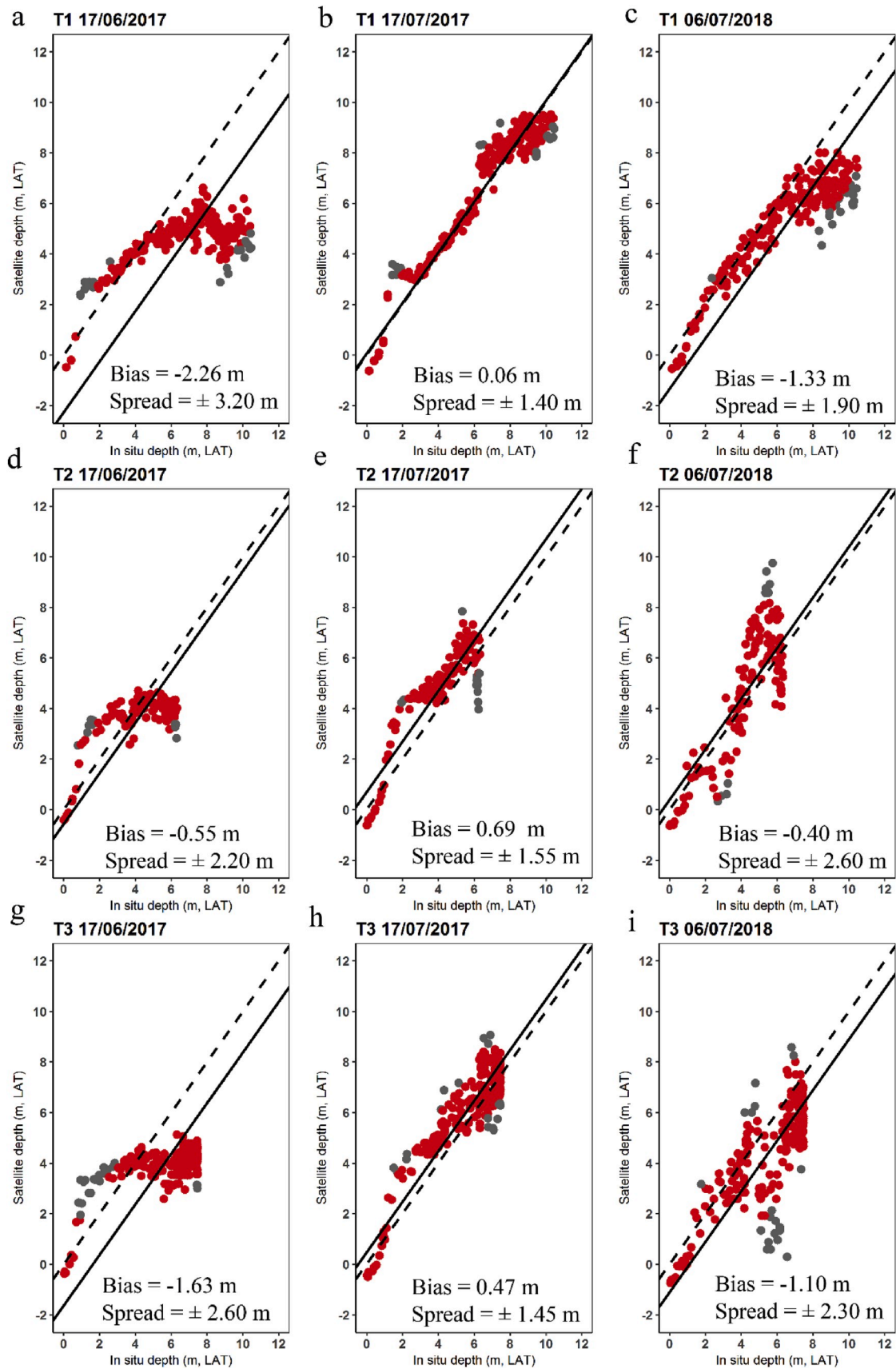
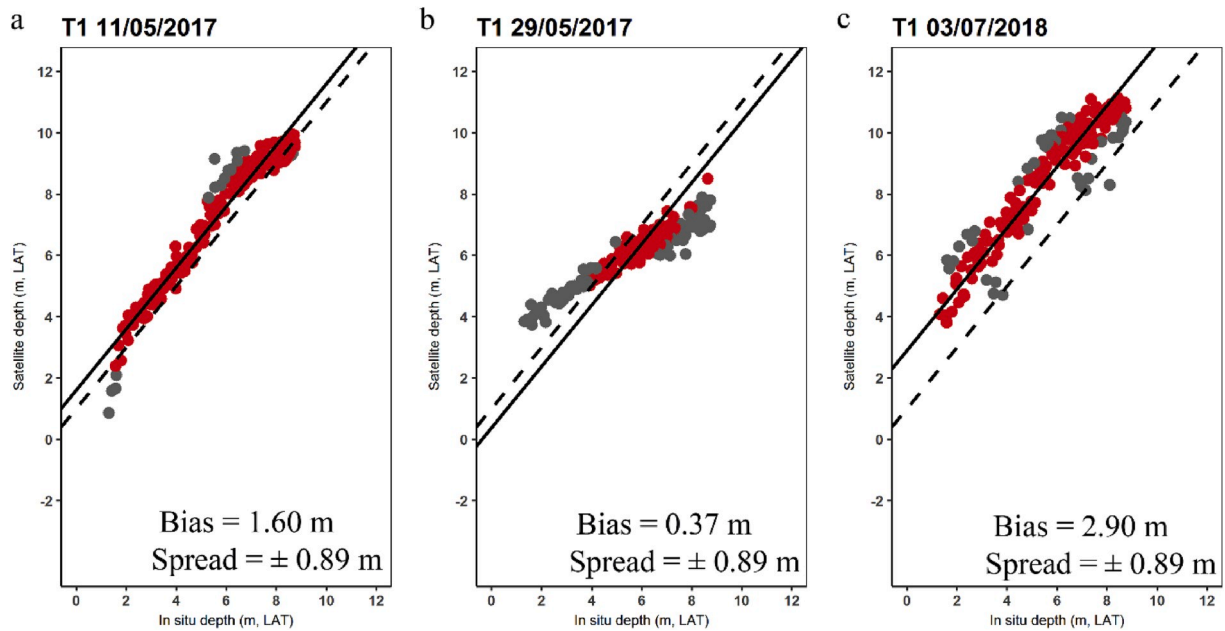
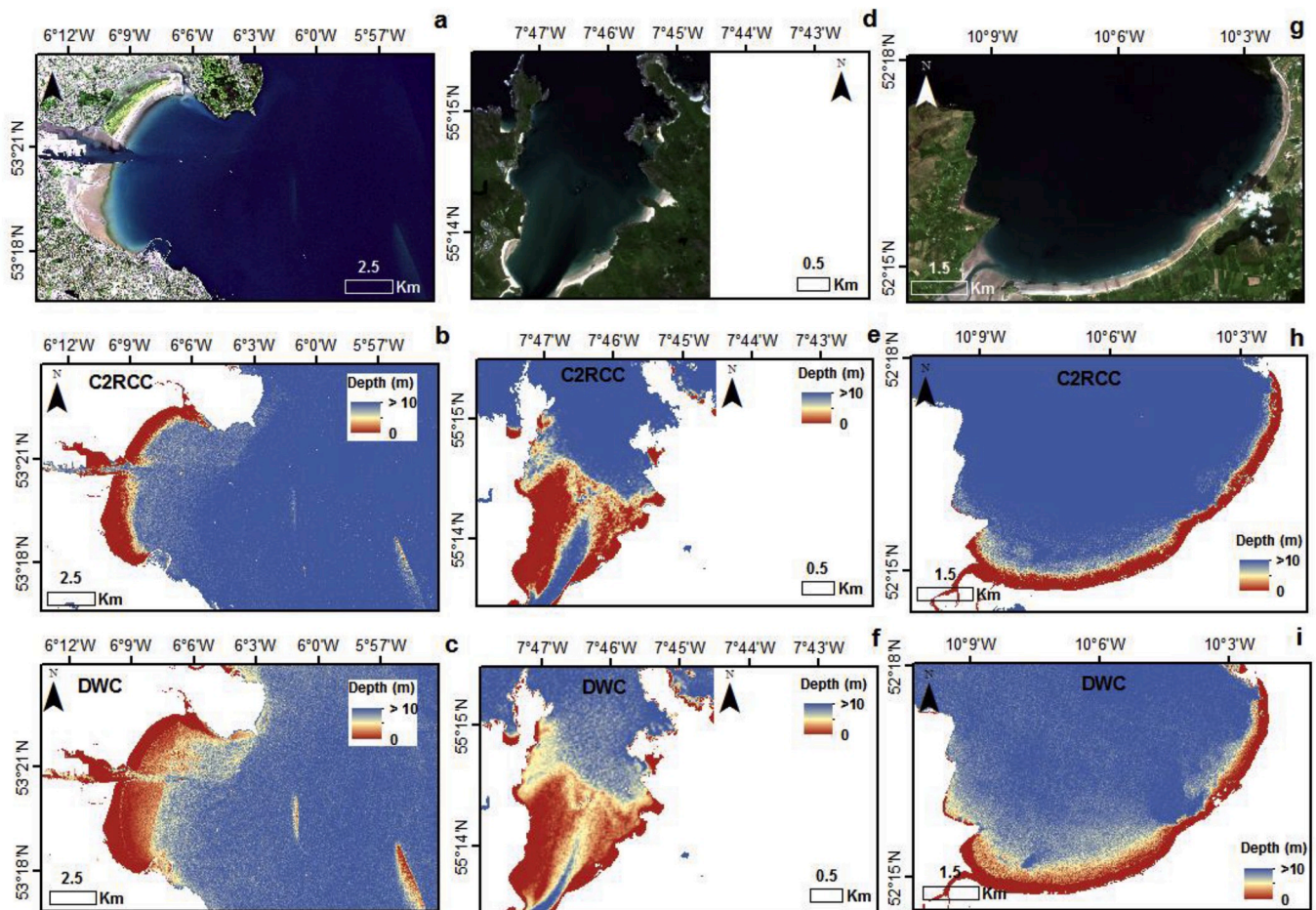


Fig. 7. Scatterplots for individual transects carried out over homogenous bottom type in Dublin Bay (see Fig. 1). Red dots fall within the 90% confidence interval. Solid line represents the bias-shifted 1:1 line and dashed line represents the 1:1 line. (For interpretation of the references to colour in this figure legend, the reader is referred to the Web version of this article.)



**Fig. 8.** Scatterplots for individual transect carried out over homogenous bottom type in Brandon Bay (see Fig. 1). Red dots fall within the 90% confidence interval. The solid line represents the bias-shifted 1:1 line and dashed line represents the 1:1 line. (For interpretation of the references to colour in this figure legend, the reader is referred to the Web version of this article.)



**Fig. 9.** Example of bathymetry maps for a-c) Dublin Bay (17/07/2017), d-f) Mulroy Bay (23/07/2017) and g-i) Brandon Bay (11/05/2019) resulting after atmospheric correction by C2RCC and DWC.

pronounced decrease in depth from the shore to the inner part of the bay, which is consistent with the more abrupt topography known to be present in this bay. This area is the most complex of the three areas considered, taking into account meteorology and water surface conditions. Brandon Bay is an exposed bay with strong swell and high turbidity. These circumstances, together with the frequent cloud coverage of the area limit the number of suitable images for satellite derived bathymetry. The influence of the discharge of the Owenmore River located in the west part of the bay could be detected in some of the bathymetric maps, especially in the ones resulting from the atmospheric correction using the DWC method (Fig. 9i). The presence of dark substrates in shallow areas close to the shore such as macroalgae resulted in the mapping of these areas as “false” deep areas in comparison with existing bathymetric mapping for the area (e.g. Fig. 9i).

### 3.5. Specific recommendations

#### 3.5.1. Atmospheric correction

Results of this study showed that atmospheric correction is a critical step in the derivation of satellite bathymetry. Although bathymetric maps produced by either correction looked reasonable at large scales (Fig. 9) specific comparisons to in situ data revealed consistent differences in performance (Fig. 4 vs. 5). While the choice of correction method was shown to have a major influence on estimated depths, variation between and even within images is likely to be contributed by atmospheric effects and the efficacy of their correction. The influence of atmospheric correction methods in MSI has already been reported in other applications related to aquatic environments (Souza-Martins et al., 2017; Hedley, 2018b; Casal et al., 2019; König et al., 2019). In this study, two different atmospheric correction methods, C2RCC and DWC, were tested. In general, the DWC approach for atmospheric correction produced more accurate and less biased satellite-derived bathymetry maps. This result is unsurprising since the DWC method is specifically designed to correct imagery for the application of the bathymetric inversion model, whereas C2RCC is a more generic method.

#### 3.5.2. Site-specific features and image selection

The analysis of the 12 scatterplot plots (with associated diagnostics) between satellite-derived depth and in situ depth revealed a high variability to the results and a clear dependence on the “quality” of image used. For example, better results can be obtained in an area of more complex waters such as Dublin Bay when the conditions are “good” (e.g. low turbidity) than in an area of more clear waters such as Mulroy Bay when the conditions are “bad” (e.g. river plume, low clouds) (e.g. Fig. 4 b and 4 h). The availability of two Sentinel-2 satellites, that in Ireland can provide a revisit time of 3 days, is of enormous importance as it increases the chance of obtaining good images in areas with significant limitations due to weather and water surface conditions. Going forward, combining multiple image analyses may be a robust way of removing outliers (Caballero and Stumpf, 2020).

The overall scatterplots (Fig. 4), location of outliers (Fig. 5) and transects (Figs. 7 and 8) revealed common features for all study areas but also inherent characteristics of each area. Satellite images after storms should be avoided for bathymetry derivation due to the production of resuspension material that strongly influences the relation between satellite signal and depth (Fig. 4 d). Areas challenging for satellite-derived bathymetry exist even in the images registered under “optimal” conditions. Local and variable turbidity events have an impact on satellite-derived bathymetry, causing an under-estimation of depth values. Dark bottom types such as rock and macroalgae also have an impact on satellite-derived bathymetry, potentially causing an overestimation of depth values. Even when the reflectances of these bottom types are included in the bathymetric model confusion can arise, simply because it is inherently difficult to determine if a dark pixel corresponds to a deep area or a shallow dark bottom. In our results, this was especially relevant in the case of Brandon Bay. Concerning these site-specific issues, it is

clear that full automation of bathymetric map production from satellite data is a challenging aim, a more practical approach for quality assurance is a careful manual interpretation based on site-specific knowledge and interpretation. However, this approach cannot be feasible in large areas.

#### 3.5.3. Empirical tuning models vs model inversion methods

Similar averages of RMSE values over the full range of depths from 0 to 10 m were obtained for Dublin Bay (RMSE = 1.60) and Mulroy Bay (RMSE = 1.66) while Brandon Bay registered the highest average RMSE value (RMSE = 2.43). The lowest RMSE value was obtained in Dublin Bay on the 17/07/2017 (RMSE = 1.00) and it is coincident with the image where the highest  $R^2$  value ( $R^2 = 0.86$ ) was found. These numbers were quite similar to the ones obtained in previous studies using empirically tuned methods like the Linear Band Model (Lyzenga, 1978, 1985; Lyzenga et al., 2006) in the same study areas. In these studies, values of  $R^2 > 0.80$  and average RMSE values of 1.05 and 0.81 were obtained for Dublin Bay and Mulroy Bay, respectively (Casal et al., 2019). These empirically tuned methods worked well in our study areas because the Sentinel-2 images were selected close to optimal conditions (e.g. low turbidity) and these areas present a homogenous bottom type. It is broadly recognised that empirically tuned algorithms can accurately retrieve bathymetry, but only in areas of constant water clarity and homogenous bottom type (Dekker et al., 2011). As mentioned before, recent works have reported potential strategies for identifying (Caballero et al., 2019) and even reducing turbidity impacts (Caballero and Stumpf, 2020). However, these empirically tuned methods require in situ training data, which is a major limitation since if such data is lacking, they cannot be used. Empirically tuned methods are also hard to verify since in situ validation data is frequently not really independent of the training data and effectively just repeats the calibration regression fit. The demonstrated accuracy of inversion approaches in the Irish coast could offer a potential solution to cover a different variety of study areas not only the ones with homogenous bottom types and water quality conditions. Where in situ data is available, this offers a genuinely independent quality assurance process. Moreover, optimization approached to calibration provide information about uncertainty and have the potential to estimate water inherent optical properties and bottom cover.

#### 3.5.4. Depth limits

Regarding the different depth ranges considered, for most images a low relationship between satellite-derived depth and in situ depth was found for depths occurring beyond 6 m. This criterion could be used to define a critical depth limit for satellite bathymetry derivation using Sentinel-2 data in these areas. Nevertheless, under good conditions with the best images, depth continues to be detectable to 10 m and possibly more, but with decreasing precision (Fig. 5). In the case of Mulroy Bay and the best Dublin Bay image, the accuracy in terms of  $R^2$  and RMSE within the 2 m depth intervals was maintained until 10 m. The depth where the relation between satellite-derived and in situ data started to deviate from 1:1 line was coincident with the results obtained using empirically tuned approaches in the same study areas (Casal et al., 2019). Moreover, these results were not so different from studies carried out in clear waters of the Australian and Caribbean coast where high absolute accuracies were obtained for bathymetry estimates down to 8–13 m (Dekker et al., 2011). Higher depths of 15 m, were reported by other authors (Hedley et al., 2018a) using Sentinel-2 data in the Great Barrier Reef. These results confirm the potential of Sentinel-2 imagery to derive medium resolution bathymetric maps, with the advantage of more cost-effective temporal coverage than offered by higher-resolution commercial sensors.

#### 3.5.5. Ranges of water column optical properties

In shallow waters, remote sensing reflectance not only depends on the absorption and scattering properties of dissolved and suspended

materials in the water column but also on the reflectivity of the bottom (Dekker et al., 2011). To take the most advantage of model inversion methods, ideally, a well-defined range of optical component values should be provided as an input of the model to generate the lowest possible uncertainty while encompassing the expected range across the site. Preliminary work for this study (not reported here) indicated that the choice of ranges for water optical properties had only a slight effect on the accuracy of the resultant bathymetry maps. However, the highest  $R^2$  and lowest RMSE and bias were reached when the defined range was the most restricted but consistent with the known ranges at the sites. For this reason, it is highly recommended to obtain information about the potential range of water column optically active constituents such as phytoplankton concentration, CDOM absorption and backscatter. In our case, this information was taken from previously published studies carried out in more general areas around the Irish coast and from the experience of the researchers. However, specific field campaigns at local level are recommended to obtain more precise and accurate results.

#### 4. Conclusions

Sentinel-2 data quality and availability for worldwide coastal regions have increased the attention of coastal managers regarding satellite-derived bathymetry applied research. This paper presents the results of a model inversion approach to predict water depths, without using existing in situ bathymetry, in optically complex waters of the Northeast Atlantic region. Practical bathymetric information is present in the results; with optimal imagery selection, depth estimates with an average bias less than 0.1 m and a spread of  $\pm 1.40$  m can be achieved up to 10 m. The accuracy of the results placed them in the Category Zones of Confidence (CATZOC) class C, providing useful information on survey planning and monitoring capabilities. Moreover, the results showed similar accuracy levels to the ones obtained using standards empirically tuned models in the same areas (Casal et al., 2019). This finding is of particular relevance as model inversion approaches might allow future modifications in critical parts of the processing chain leading to improved results. Such improvements can be part of the atmospheric correction step, sea surface corrections or better containing the optical water constituents. Besides, other non-model specific improvements that come from processing multiple datasets and applying a median filter may help to reduce the bias.

Furthermore, the assessment carried out in this work provides key points in the understanding of a model inversion approach to derive bathymetric data in similar optically complex waters. The transferability of these methods between locations is a challenge, and the best accuracies will be expected when local algorithms are applied. As shown here, any specific site will have its own anomalies and features that will introduce spatial artefacts into the bathymetry analysis. Visual interpretation and manual intervention in map production can remain a necessary step. Nevertheless, this process becomes more manageable, since the technical capabilities such as spatial resolution and revisit time offered by Sentinel-2, together with its cost-effectiveness, present many advantages to select optimal images, a critical step in the extraction of optimal bathymetric values.

#### Declaration of competing interest

The authors declare that they have no known competing financial interests or personal relationships that could have appeared to influence the work reported in this paper.

#### CRedit authorship contribution statement

**Gema Casal:** Funding acquisition, Project administration, Conceptualization, Methodology, Formal analysis, Visualization, Writing - original draft, Writing - review & editing. **John D. Hedley:** Conceptualization, Methodology, Writing - review & editing. **Xavier Monteys:**

Conceptualization, Methodology, Writing - review & editing. **Paul Harris:** Writing - review & editing. **Conor Cahalane:** Writing - review & editing. **Tim McCarthy:** Project administration, Writing - review & editing.

#### Acknowledgements

This work was supported by the Geological Survey Ireland/DCCAE Postdoctoral Fellowship Programme under the grant No. 2016-PD-005. Funding was also provided by Biotechnology and Biological Sciences Research Council (BBSRC) grants BBS/E/C/000J0100; BBS/E/C/000I03320 and BBS/E/C/000I0330. Multibeam data were provided by the INFOMAR Programme. Tide data were obtained through the Irish National Tide Gauge Network. ESA and Copernicus are thanked for Sentinel-2 imagery. Authors thank the two anonymous reviewers that with their comments helped to improve the present manuscript.

#### Appendix A. Supplementary data

Supplementary data to this article can be found online at <https://doi.org/10.1016/j.ecss.2020.106814>.

#### References

- Antoine, D., Morel, A., 1999. A multiple scattering algorithm for atmospheric correction of remotely sensed ocean colour (MERIS instrument): principle and implementation for atmospheres carrying various aerosols including absorbing ones. *Int. J. Rem. Sens.* 20, 1875–1916.
- Brockmann, C., Doerffer, R., Peters, M., Stelzer, K., Embacher, S., Ruescas, A., 2016. Evolution of the C2RCC Neural Network for Sentinel 2 and 3 for the retrieval of ocean colour products in normal and extreme optically complex waters. In: *Proceedings of the Living Planet Symposium 2016*, Prague, Czech Republic, pp. 9–13. May 2016.
- Bowers, D.G., Roberts, E.M., White, M., Moate, B.D., 2013. Water masses, mixing, and the flow of dissolved organic carbon through the Irish Sea. *Contin. Shelf Res.* 58, 12–20.
- Brando, V.E., Anstee, J.M., Wettle, M., Dekker, A.G., Phinn, S.R., Roelfsema, C., 2009. A physics based retrieval and quality assessment of bathymetry from suboptimal hyperspectral data. *Rem. Sens. Environ.* 113, 755–770.
- Brooks, P.R., Nairn, R., Harris, M., Jeffrey, D., Crowe, T.P., 2016. Dublin port and Dublin bay: reconnecting with nature and people. *Regional Studies in Marine Science*. <https://doi.org/10.1016/j.rsma.2016.03.007>.
- Caballero, I., Stumpf, R., Meredith, A., 2019. Preliminary assessment of turbidity and chlorophyll impact on bathymetry derived from Sentinel-2A and Sentinel-3A satellites in South Florida. *Rem. Sens.* 11 (6), 645.
- Caballero, I., Stumpf, R., 2020. Towards routine mapping of shallow bathymetry in environments with variable turbidity: contribution of Sentinel-2A/B satellites mission. *Rem. Sens.* 12 (3), 451.
- Cahalane, C., Magee, A., Monteys, X., Casal, G., Hanafin, J., Harris, P., 2019. A comparison of Landsat 8, RapidEye and Pleiades products for improving empirical predictions of satellite-derived bathymetry. *Rem. Sens. Environ.* 233, 111414.
- Cahalane, C., Hanafin, J., Monteys, M., 2017. Improving satellite-derived bathymetry using spatial regression algorithms. *Hydro Int.* 16–19.
- Casal, G., Harris, P., Monteys, X., Hedley, J.D., Cahalane, C., McCarthy, T., 2020. Understanding satellite derived bathymetry using Sentinel 2 imagery and spatial prediction models. *GIScience Remote Sens.* 57 (3), 271–286. <https://doi.org/10.1080/15481603.2019.1685198>.
- Casal, G., Monteys, M., Hedley, J.D., Harris, P., Cahalane, C., McCarthy, T., 2019. Assessment of empirical algorithms for bathymetry extraction using Sentinel-2 data. *Int. J. Rem. Sens.* 40 (8), 2855–2879.
- Collings, S., Botha, E.J., Anstee, J., Campbell, N., 2018. Depth from satellite images: depth retrieval using a stereo and radiative transfer-based hybrid method. *Rem. Sens.* 10 (8), 1247. <https://doi.org/10.3390/rs10081247>.
- Coveney, S., Monteys, X., 2011. Integration potential of INFOMAR airborne LIDAR bathymetry with external onshore LIDAR data sets. *J. Coast Res.* 62, 19–29.
- Dekker, A.G., Phinn, S.R., Anstee, J., Bissett, P., Brando, V.E., Casey, B., Fearn, P., Hedley, J.D., Klonowski, W., Lee, Z.P., Lynch, M., Lyons, M., Mobley, C., Roelfsema, C., 2011. Intercomparison of shallow water bathymetry, hydro-optics, and benthos mapping techniques in Australian and Caribbean coastal environment. *Limnol Oceanogr. Methods* 9, 396–425.
- Doerffer, R., Schiller, H., 2007. The MERIS case 2 water algorithm. *Int. J. Rem. Sens.* 28 (3), 517–535.
- Dyer, K.R., 1973. *Estuaries: A Physical Introduction*. Wiley, Chichester.
- Emde, C., Barlakas, V., Cornet, C., Evans, F., Korin, S., Ota, Y., Labonnote, L.C., Lyapustin, A., Macke, A., Mayer, B., Wendisch, M., 2015. IPRT polarized radiative transfer model intercomparison project – phase A. *J. Quant. Spectrosc. Ra.* 164, 8–36. <https://doi.org/10.1016/j.jqsrt.2015.05.0072015>.
- ESA (European Space Agency), 2018. Sentinel-2 Data Quality Report. Ref: S2-PDGS-MPC-DQR.

- Eugenio, F., Marcello, J., Martin, J., 2015. High-resolution maps of bathymetry and benthic habitats in shallow-water environments using multispectral remote sensing imagery. *IEEE Trans. Geosci. Rem. Sens.* 53, 3539–3549.
- Eugenio, F., Marcello, J., Martin, J., Rodríguez-Esparragón, J.G., 2017. Benthic habitat mapping using multispectral high-resolution imagery: evaluation of shallow water atmospheric correction techniques. *Sensors* 17, 2639.
- Evagorou, E., Mettas, C., Agapiou, A., Themistocleous, K., Hadjimitsis, D., 2019. Bathymetric maps from multi-temporal analysis of Sentinel-2 data: the case study of Limassol, Cyprus. *Adv. Geosci.* 45, 397–407.
- Gamito, R., Pita, C., Teixeira, C., Costa, M.J., Cabral, H.N., 2019. Trends in landings and vulnerability to climate change in different fleet components in the Portuguese coast. *Fish. Res.* 181, 93–101.
- Gao, J., 2009. Bathymetric mapping by means of remote sensing: methods, accuracy and limitations. *Prog. Phys. Geogr.* 33 (1), 103–116.
- Garaba, S., Voß, D., Zielinski, O., 2014. Physical, bio-optical state and correlations in north western European shelf seas. *Rem. Sens.* 6 (6), 5042–5066.
- Goodman, J.A., Lee, A., Ustin, S.L., 2008. Influence of atmospheric and sea-surface corrections on retrieval of bottom depth and reflectance using a semi-analytical model: a case study in Kaneohe Bay, Hawaii. *Appl. Optic.* 47 (28), F1–F11.
- Gordon, H.R., Morel, A.Y., 1983. Remote assessment of ocean color for interpretation of satellite visible imagery. In: *A Review of Lecture Notes on Coastal and Estuarine Studies*. Springer-Verlag, New York.
- Halpern, B.S., Walbridge, S., Selkoe, K.A., Kapperl, C.V., Micheli, F., D'Agrosa, C., Bruno, J.F., Casey, K.S., Ebert, C., Fox, H.E., Fujita, R., Heinemann, D., Lenihan, H.S., Madin, E.M.P., Perry, M.T., Selig, E.R., Spalding, M., Steneck, R., Watson, R., 2018. A global map of human impact on marine ecosystems. *Science* 319, 948–952.
- Hamylton, S.M., Hedley, J., Beaman, R.J., 2015. Derivation of high-resolution bathymetry from multispectral satellite imagery: a comparison of empirical and optimisation methods through geographical error analysis. *Rem. Sens.* 7, 16257–16273.
- Hedley, J., 2018. Atmospheric correction of Sentinel-2 and Landsat 8 for satellite derived bathymetry. In: *Ocean Optics XXIV Conference*, Dubrovnik, Croatia. October 7–12.
- Hedley, J.D., Harborne, A.R., Mumby, P.J., 2005. Simple and robust removal of sun glint for mapping shallow-water benthos. *Int. J. Rem. Sens.* 26, 2107–2112.
- Hedley, J.D., Roelfsema, C., Brando, V., Giardino, C., Kutser, T., Phinn, S., Mumby, P.J., Barrilero, O., Laporte, J., Koetz, B., 2018. Coral reef applications of Sentinel-2: coverage, characteristics, bathymetry and benthic mapping with comparison to Landsat 8. *Rem. Sens. Environ.* 216, 598–614.
- Hedley, J.D., Roelfsema, C., Phinn, S., 2010. Propagating uncertainty through a shallow water mapping algorithm based on radiative transfer model inversion. In: *Anchorage, A.K. (Ed.), Proceedings of the Ocean Optics XX Conference*. USA, 27 September–1 October 2010.
- Hedley, J.D., Roelfsema, C., Koetz, B., Phinn, S., 2012. Capability of the Sentinel 2 mission for tropical coral reef mapping and coral bleaching detection. *Rem. Sens. Environ.* 120, 145–155.
- Hedley, J.D., Roelfsema, C., Phinn, S.R., 2009. Efficient radiative transfer model inversion for remote sensing applications. *Rem. Sens. Environ.* 113, 2527–2532.
- Hedley, J.D., Russell, B., Randolph, K., Dierssen, H., 2016. A physics-based method for the remote sensing seagrasses. *Rem. Sens. Environ.* 174, 134–147.
- König, M., Hieronymi, M., Oppelt, N., 2019. Application of Sentinel-2 MSI in Arctic Research: evaluating the performance of atmospheric correction approaches over Arctic sea ice. *Front. Earth Sci.* 7, 22.
- Lee, Z., Carder, K.L., Mobley, C.D., Steward, R.G., Patch, J.S., 1998. Hyperspectral remote sensing for shallow waters. I. A semianalytical model. *Appl. Optic.* 37, 6329–6338.
- Lee, Z., Carder, K.L., Mobley, C.D., Steward, R.G., Patch, J.F., 1999. Hyperspectral remote sensing for shallow waters: 2. Deriving bottom depths and water properties by optimization. *Appl. Optic.* 38, 3831–3843.
- Lee, Z., Kendall, L.C., Chen, R.F., Peacock, T.G., 2001. Properties of the water column and bottom derived from airborne visible imaging spectrometer (AVIRIS) data. *Journal of Geophysical Research-Oceans* 106, 11639–11651.
- Lipiec, E., Ruggiero, P., Mills, A., Serafin, K.A., Bolte, J., Corcoran, P., Stevenson, J., Zanocco, C., Lach, D., 2018. Mapping out climate change: assessing how coastal communities adapt using alternative future scenarios. *J. Coast Res.* 34 (5), 1196–1208.
- Lyons, M., Phinn, S., Roelfsema, C., 2011. Integrating quickbird multispectral satellite and field data: mapping bathymetry, seagrass cover, seagrass species and change in moreton bay, Australia in 2004 and 2007. *Rem. Sens.* 3 (1), 42–64.
- Lyzenga, D.R., 1978. Passive remote sensing techniques for mapping water depth and bottom features. *Appl. Optic.* 17, 379–383.
- Lyzenga, D.R., 1985. Shallow-water bathymetry using combined LiDAR and passive multispectral scanner data. *Int. J. Rem. Sens.* 6, 115–125.
- Lyzenga, D.R., Malinas, N.P., Tanis, F.J., 2006. Multispectral bathymetry using a simple physically based algorithm. *IEEE Trans. Geosci. Rem. Sens.* 44, 2251–2259.
- Monteys, X., Harris, P., Caloca, S., Cahalane, C., 2015. Spatial prediction of coastal bathymetry based on multispectral imagery and multibeam data. *Rem. Sens.* 7, 13782–13806.
- Moreno-Navas, J., Telfer, T.C., Ross, L.G., 2011. Application of 3D hydrodynamic and particle tracking models for better environmental management of finfish culture. *Continent. Shelf Res.* 31, 675–684.
- O'Boyle, S., Silke, J., 2010. A review of phytoplankton ecology in estuarine and coastal waters around Ireland. *J. Plankton Res.* 32 (1), 99–118.
- O'Higgins, T.G., Wilson, J.G., 2005. Impact of the river Liffey discharge on nutrient and chlorophyll concentrations in the Liffey estuary and Dublin Bay (Irish Sea). *Estuarine, Coastal and Shelf Science* 64, 323–334.
- Pacheco, A., Hortan, J., Loureiro, C., Ferreira, O., 2015. Retrieval of nearshore bathymetry from Landsat 8 images: a tool for coastal monitoring in shallow waters. *Rem. Sens. Environ.* 159, 102–116.
- Sagawa, T., Yamashita, Y., Okumura, T., 2019. Satellite derived bathymetry using machine learning and multi-temporal satellite images. *Rem. Sens.* 11, 1155.
- Shettle, E.P., Fenn, R.W., 1975. Models of the atmospheric aerosols and their optical properties. *AGARD Conference Proc. No. 183, Opt. Propagation in the Atmosphere*. In: 16, Presented at the Electromagnetic Wave Propagation Panel Symp. Lingby, Denmark, pp. 2.1–2.2, 27–31 Oct. 1975, available from NTIS, Acc. No. N76-29817.
- Souza-Martins, V., Barbosa, C., De Carvalho, L., Jorge, D., Lobo, F., Novo, E.M.L.d.M., 2017. Assessment of atmospheric correction methods for sentinel-2 MSI images applied to amazon floodplain lakes. *Rem. Sens.* 9, 322.
- Telfor, T., Robinson, K., 2003. Environmental quality and carrying capacity for aquaculture in. In: *Mulroy Bay Co. Donegal. Marine Environmental and Health Series*, vol. 9. Marine Institute, Ireland. ISSN, p. 103, 1649 - 0053.
- Traganos, D., Poursanidis, D., Aggarwal, B., Chrysoulakis, N., Renartz, P., 2018. Estimating satellite-derived bathymetry (SDB) with google earth engine and sentinel-2. *Rem. Sens.* 10 (6), 859. <https://doi.org/10.3390/rs10060859>.
- Wölf, A.C., Snaith, H., Amirebrehimi, S., Devey, C.W., Dorschel, B., Ferrini, V., Huvenne, V.A.I., Jakobsson, M., Jencks, J., Johnston, G., Lamarche, G., Mayer, L., Millar, D., Pedersen, T.H., Picard, K., Reitz, A., Schmitt, T., Visbeck, M., Weatherall, P., Wigley, R., 2019. Seafloor mapping – the challenge of a truly global ocean bathymetry. *Frontiers in Marine Science* 6, 283. <https://doi.org/10.3389/fmars.2019.00283>.